

## INFLUENCE OF HIGH COMPRESSION RATIO AND EXCESS AIR RATIO ON PERFORMANCE AND EMISSIONS OF NATURAL GAS FUELLED SPARK IGNITION ENGINE

by

Mario SREMEC<sup>a\*</sup>, Mladen BOŽIĆ<sup>a</sup>, Ante VUČETIĆ<sup>a</sup>, and Darko KOZARAC<sup>a</sup>

<sup>a</sup> Department of Internal Combustion Engines and Mechanical Handling Equipment, Faculty of Mechanical Engineering and Naval Architecture, Zagreb, Croatia

Original scientific paper

<https://doi.org/10.2298/TSCI182205???O>

*Compressed natural gas is in automotive industry recognized as one of the "cleanest" fossil fuels which can be used in internal combustion engines with a number of benefits. Since natural gas has much higher octane rating than gasoline it is expected that higher compression ratios can be used. The goal of the research is to determine the change of performance of spark ignited engine with the increase of compression ratio to values similar to compression ignited engine while keeping the exhaust emissions on the acceptable level and avoiding knock combustion. Measurements are performed at compression ratios 12, 16 and 18 at three different values of air excess ratio. Methane with known composition from a pressure cylinder is used instead of natural gas and the results are comprised of indicating results (in-cylinder and intake pressure in a crank angle space), emissions, temperatures and mass flows on various intake and exhaust positions. Analysis of results shows high influence of compression ratio and excess air ratio on combustion, performance and exhaust gas emissions.*

*Key words: methane, spark ignition engine, compression ratio, natural gas, compressed natural gas*

### Introduction

Steady growth of industry and world population leads to a higher energy consumption, which then leads to the increase of greenhouse gases emissions. Most of the energy still comes from the fossil fuels and in order to decrease the harmful influence of using fossil fuels, governments around the world implement regulations that restrict exhaust gas emissions. Transport sector is recognized as the second major source of pollution [1] and in order to fulfil the requirements set by regulations and to decrease harmful effect to the environment, there are a couple of options available: developing different combustion techniques and exhaust gas after treatment systems or implementing alternative and more acceptable fuels.

Previous research in the field of alternative fuels for internal combustion (IC) engines show a great potential of the natural gas (NG) with respect to the performance and environmental influence. Besides being an alternative fuel, by using the NG instead of conventional fuels (diesel and gasoline) in internal combustion engine it is possible to obtain similar efficiency and to simultaneously reduce non-methane hydrocarbon (NMHC), carbon monoxide (CO), nitrous oxide (NO<sub>x</sub>) and particulate matter (PM) emissions [2]. Although natural gas is also a fossil fuel, because of its chemical composition it produces significantly less CO<sub>2</sub>

\* Corresponding author; e-mail: mario.sremec@fsb.hr

compared to the gasoline or diesel fuel (up to 25% less) [3]. Further advantage of NG in comparison to gasoline is the high octane number (ON = 120) which allows the use of natural gas in spark ignition (SI) engines with higher compression ratio (CR). In IC engines NG can be used as single fuel in SI engines and in dual-fuel combustion operation (diesel + NG) in compression ignition (CI) engines. In CI engine, dual-fuel operation is required because of the high auto ignition temperature and low reactivity of NG [3].

Most of available experimental research of using natural gas in SI engines is performed on conventional gasoline engines and most of presented results show comparison of performances between gasoline and NG fuel. Engine operation with NG results in some advantages compared to the operation with gasoline fuel, but also with some disadvantages. In [4] authors showed that the SI engine fuelled with NG produces 18.5% less power compared to the gasoline due to the lower volumetric efficiency, which is caused by the fact that NG has lower molar mass and therefore displaces more air in the intake port. Comparison between NG and gasoline in retrofitted gasoline vehicle (Compression ratio = 9.2) is given in [5]. Authors showed that engine fuelled by NG has lower power and lower brake specific fuel consumption (BSFC), emits less CO and HC emissions, but also 33% more NO<sub>x</sub> emission, compared to the engine fuelled by gasoline. Similar conclusions were obtained in [6] where SI engine that had compression ratio of 9.5 was tested. An effective method for reducing NO<sub>x</sub> emissions and improving thermal efficiency is a lean burn strategy, presented in [7, 8], but an ultra-lean operation ( $\lambda > 2$ ) can result in misfire and unstable operation [8].

The experimental study of influence of compression ratio [9] tested three different compression ratios 8.5, 10.5 and 12.5 and showed that the increase of heat release rate, power output, thermal efficiency and NO<sub>x</sub> emission is obtained with the increase of compression ratio. At excess air ratio near the misfire limit hydrocarbon emission also increases with the increase of compression ratio. In [10] the influences of EGR and three-way catalyst (TWC) on emissions of spark ignited natural gas heavy-duty Euro VI engine (compression ratio = 11.5) are shown and the results show that the engine without TWC cannot satisfy EURO VI NO<sub>x</sub> emission standard while by using the TWC NO<sub>x</sub> emission drops significantly below the allowed value. Authors in [11, 12] show air fuel ratio (AFR) and exhaust gas recirculation (EGR) dilution effects as well as start of injection and spark timing effects on combustion phasing, fuel consumption, knock and emissions of spark ignited direct injection natural gas single cylinder engine with compression ratio 14. Direct injection shows better cycle efficiency and extends the lean limits which further extended the knock limit. AFR and EGR were effective parameters in controlling knock and decreasing NO<sub>x</sub> emission. Comparison of influence of compression ratios (10.5 and 11.5) in heavy-duty spark ignited CNG engine is performed in [13] where the improvement in thermal efficiency with increased compression ratio is shown, but the increase of CR also leads to higher NO<sub>x</sub> emission. In [14] the comparison of four compression ratios in spark ignition natural gas engine is made (CR between 8 and 14.7) with the emphasis on NO<sub>x</sub> and HC emissions. They noticed the increase in NO<sub>x</sub> and HC emission with the increase of compression ratio for running with the same spark timing, but with optimised spark timing the engine could achieve high efficiency with low emissions.

The overview of the previous research indicates a lack of experimental results for natural gas fuelled SI engines with compression ratio higher than 14.7 (in the CI engine range). The research on engines with higher compression ratio is mostly performed in dual-fuel combustion operation. Since higher compression ratio could lead to higher efficiency and could enable operation with leaner mixtures, the main objectives of this research are to experimentally investigate behaviour of SI engine fuelled by natural gas at higher compression

ratios and at different mixture dilution levels. The experimental tests were performed at three different compression ratios, one compression ratio similar to conventional gasoline engine (CR = 12) and two compression ratios similar to conventional diesel engine (CR = 16 and CR = 18) and at three values of air excess ratio ( $\lambda$ ),  $\lambda = 1$ ,  $\lambda = 1.2$  and  $\lambda = 1.4$ . These values of air excess ratio are chosen because the literature review showed that the increase of lambda decreases NO<sub>x</sub> emission, while lambda higher than 1.54 ( $\phi < 0.65$ ) causes unstable engine operation in the natural gas fuelled SI engine [15].

#### Experimental setup and test cases

The presented study was performed on the experimental setup located in the Laboratory of IC engines and motor vehicles at the Faculty of Mechanical Engineering and Naval Architecture in Zagreb that has been built by using Hatz 1D81 engine [16] as a basis. Engine properties are given in tab. 1. For the proposed research experimental engine was converted from CI engine to SI engine operation. Instead of diesel fuel injector, spark plug is mounted into the cylinder head. Engine is also equipped with the high pressure sensor (AVL GH14DK) mounted on the cylinder head and low pressure sensor (AVL LP11DA) mounted in front of the intake valve. The change from original compression ratio (20.5) to compression ratio of 18 and 16 is obtained by addition

of thicker cylinder head gaskets, while the compression ratio of 12 is achieved by changing (machining) the height of the piston. For the preparation of the fuel mixture the gas injector is installed into the intake pipe, close to the intake valve. Instead of natural gas, pure methane (99.95% vol.) from the pressure bottle is used as a fuel. The fuel flow is controlled by appropriate opening of the fuel injector and the flow is measured by Coriolis flowmeter Endress+Hauser Promass A100. Air mass flow is measured by a flow meter TSI 2017 which is placed in front of the settling tank and used for smoothing of the flow since the setup has only one cylinder. The oxygen concentration (lambda value) and NO<sub>x</sub> concentration are measured by in line ECM NO<sub>x</sub> 5210T analyser (NO<sub>x</sub> measurement accuracy:  $\pm 20$  ppm from 200 to 1,000 ppm,  $\pm 2\%$  elsewhere), while for measurement of CO, CO<sub>2</sub> and total hydrocarbon (THC) the standard methods for measurement were used; for CO and CO<sub>2</sub> non dispersive infra-red analyser Environment S.A. MIR 2M (accuracy:  $< 1\%$ ) and for THC flame ionisation detector (FID) analyser Environment S.A. GRAPHITE 52M (accuracy:  $< 1\%$ ). Figure 1 shows schematic diagram of the experimental setup.

**Table 1. Specifications of the test engine**

Item	Specification
Type	Single cylinder
Piston displacement	667 cm <sup>3</sup>
Stroke	4-stroke
Bore	100 mm
Stroke	85 mm
Connecting rod length	127 mm
Compression ratio	Adjustable (original 20.5)

of thicker cylinder head gaskets, while the compression ratio of 12 is achieved by changing (machining) the height of the piston. For the preparation of the fuel mixture the gas injector is installed into the intake pipe, close to the intake valve. Instead of natural gas, pure methane (99.95% vol.) from the pressure bottle is used as a fuel. The fuel flow is controlled by appropriate opening of the fuel injector and the flow is measured by Coriolis flowmeter Endress+Hauser Promass A100. Air mass flow is measured by a flow meter TSI 2017 which is placed in front of the settling tank and used for smoothing of the flow since the setup has only one cylinder. The oxygen concentration (lambda value) and NO<sub>x</sub> concentration are measured by in line ECM NO<sub>x</sub> 5210T analyser (NO<sub>x</sub> measurement accuracy:  $\pm 20$  ppm from 200 to 1,000 ppm,  $\pm 2\%$  elsewhere), while for measurement of CO, CO<sub>2</sub> and total hydrocarbon (THC) the standard methods for measurement were used; for CO and CO<sub>2</sub> non dispersive infra-red analyser Environment S.A. MIR 2M (accuracy:  $< 1\%$ ) and for THC flame ionisation detector (FID) analyser Environment S.A. GRAPHITE 52M (accuracy:  $< 1\%$ ). Figure 1 shows schematic diagram of the experimental setup.

Engine tests were performed at three different engine speeds (1,200 min<sup>-1</sup>, 1,600 min<sup>-1</sup>, 2,000 min<sup>-1</sup>) and at three different excess air ratios ( $\lambda = 1$ ,  $\lambda = 1.2$ ,  $\lambda = 1.4$ ). All tests were performed at wide open throttle (WOT) position with ambient conditions at the air inlet. To determine the optimal spark timing (ST) for maximum brake torque (MBT) [17], spark sweep process was performed for every predefined operating point (compression ratio, engine speed and air fuel ratio). During measurements of all operating points the ambient conditions (temperature, ambient pressure, humidity, etc.) were very similar. Inlet air temperature was within 3 °C in all operating points, while intake pressure varied from 0.97 to 0.99 bars.

Thermal efficiency and the rate of heat release (RoHR) are calculated from the measured values by using an in-house developed code. Measured pressure of each individual cycle was smoothed by using a Savitzki-Golay filter with 19 points and the calculation of RoHR is based on the first law of thermodynamics and includes changes of mixture composition and properties, with properties calculated by using NASA polynomials, the calculation of wall heat losses by Woschni model and the calculation of blow by losses. More details about the calculation of RoHR can be found in [18]. From calculated RoHR the code calculates timings of specific mass fraction burned as CA5, CA10, CA50, etc. These values are calculated for each individual cycle and then averaged over 300 consecutive cycles.

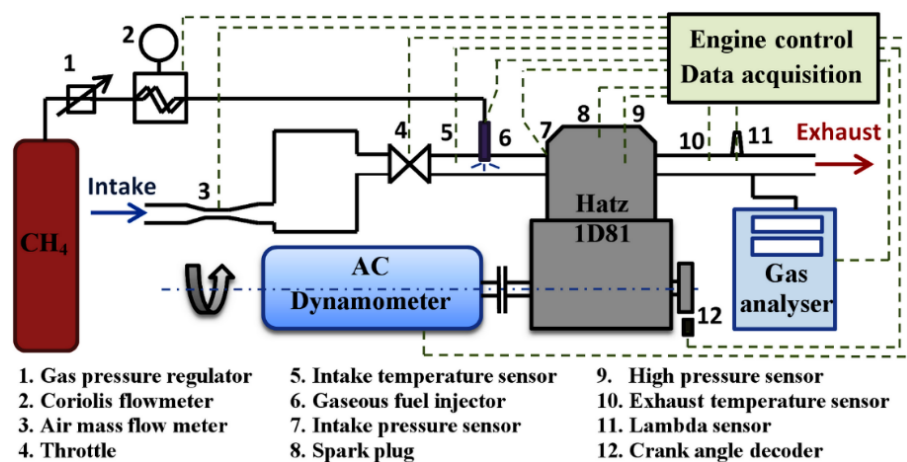


Figure 1. Schematic diagram of experimental setup

## Results and discussions

As described in the previous section, for every engine speed, compression ratio and excess air ratio a spark timing sweep was performed in order to determine the optimal combustion phasing, with criteria of maximum efficiency. With advancing the spark timing, the maximum IMEP was achieved before knock occurred in all the cases.

Figure 2 shows the IMEP and indicated efficiency for the spark timing sweep at compression ratio 18 and stoichiometric excess air ratio. From the presented results the optimum spark timings for CR = 18 and  $\lambda = 1$  are ST = 9 °CA BTDC, ST = 12 °CA BTDC and ST = 12 °CA BTDC for 1,200, 1,600 and 2,000  $\text{min}^{-1}$ , respectively.

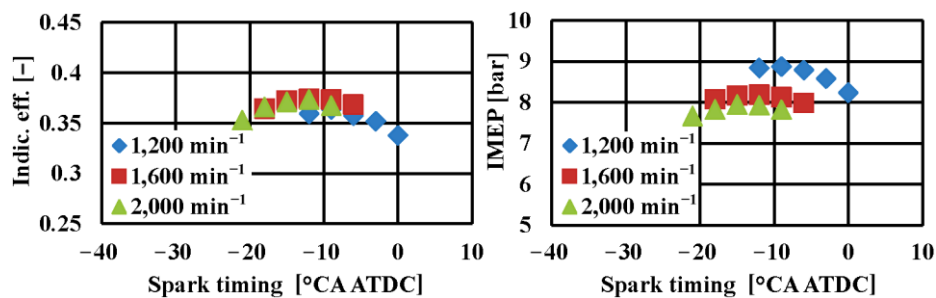


Figure 2. Spark timing sweep at CR = 18 and  $\lambda = 1$ , indicated efficiency (left); IMEP (right)

With defined optimal spark timings for every set of conditions it is possible to compare the performance results at optimal operating conditions. Figure 3 compares the results of IMEP at different engine speeds, compression ratios and excess air ratios at optimal combustion phasing. It can be seen that with the increase of compression ratio from CR = 12 to the compression ratio of conventional diesel engine (CR = 16) the IMEP also increases, but further increase to the CR = 18 results in a significant drop in IMEP. This drop in IMEP is more pronounced at higher excess air ratio and higher engine speed. The change in IMEP is mostly the result of changes in indicated efficiency which will be discussed separately. The results also show that the IMEP obtained with stoichiometric mixture are higher than the ones obtained with lean mixtures, which is caused by the less energy supply from fuel of the lean mixture. Also, trends show a decrease in IMEP value by the increase of engine speed due to the decreases in volumetric efficiency of the engine.

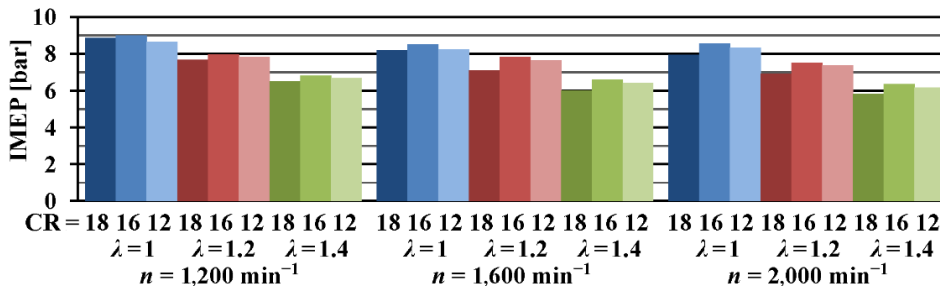


Figure 3. IMEP in dependence of CR, lambda and engine speed

The changes of spark timing, of CR and of excess air ratio causes the changes in ignition delay, and in combustion duration since the conditions at the spark discharge change. Figure 4 shows ignition delay while fig. 5 shows combustion duration for all operating points. Ignition delay is calculated as a difference between CA5 and spark timing, where the spark timing is a crank angle at which the spark discharges between the electrodes. The combustion duration is defined as the difference between CA90 and CA10.

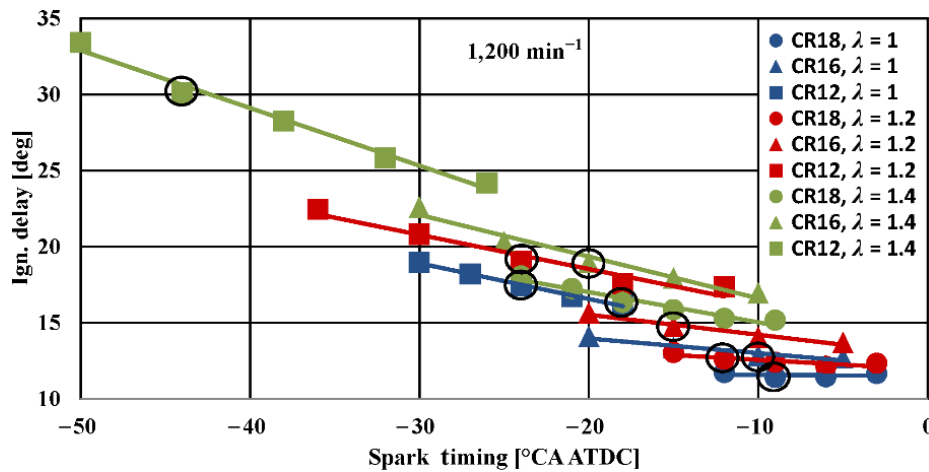


Figure 4. Ignition delay vs. spark timing

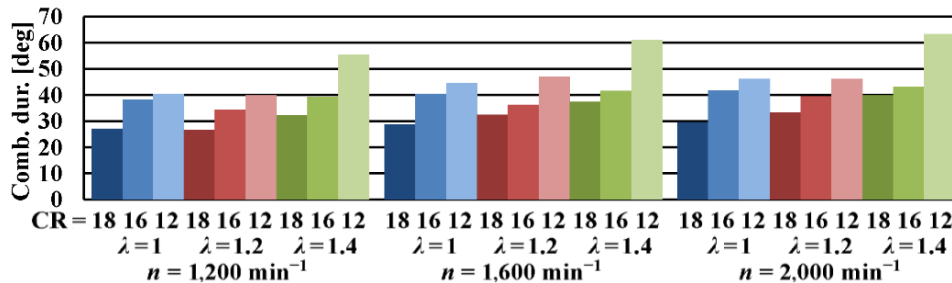


Figure 5. Combustion duration in dependence of CR, lambda and engine speed

The ignition delay shown in Figure 4 is plotted against the spark timing. For better understanding of the influence of compression ratio and lambda on ignition delay, the results are plotted for all spark sweep points. Optimum points for every CR and lambda are marked with a circle. While it can be noticed that the compression ratio and the excess air ratio have influence on ignition delay it seems that the spark timing has the largest influence on ignition delay with more advanced spark timing leading to longer ignition delay. Therefore, since the optimal spark timing change between compression ratio and excess air ratio this leads to the changes in ignition delay. Consequently with the increase of excess air ratio and a decrease of CR the increase of ignition delay is obtained, where this increase is small except for the case with the lowest CR and highest excess air ratio. The similar trend is obtained at other engine speeds, with the only difference that values of ignition delay are higher at increased engine speed.

With respect to combustion duration the results show that the increase of compression ratio decreases combustion duration at all lambda values and all engine speeds. Engine speed also has influence on combustion duration. Higher engine speed increases combustion duration in all test cases but its influence is most significant at lower CR and higher lambda ( $\lambda = 1.4$ ). By combining results of ignition delay and combustion duration one can notice that at higher lambda and lower CR the increase of combustion duration and ignition delay is very large which then leads to the requirement of very early spark timing to maintain combustion phasing. But, excessively advanced spark timing can lead to misfire as the spark discharge is at low temperature and pressure.

The consequence of changes in combustion profile and in thermodynamic cycle caused by the changes in CR, engine speed and excess air ratio is a change in engine efficiency. The indicated efficiencies of all optimal cases are shown in fig. 6. Results show significantly higher indicated efficiency at higher compression ratios (16 and 18) compared to the compression ratio 12 for the same excess air ratio value. The results also show that at CR = 12 the increase of excess air ratio generally increases indicated efficiency, while at CR = 16 and CR = 18 the increase of excess air ratio from 1 to 1.2 leads to increase of indicated efficiency due to the higher combustion efficiency, which is confirmed by the low level of CO emission and lower or equal levels of THC emission, and lower thermal losses because of lower in-cylinder temperature. Further increase of excess air ratio from 1.2 to 1.4 decreases indicated efficiency due to the slower flame propagation through lean mixture which results in lower combustion efficiency. In these cases crevices also have significant influence. By analysing results at constant excess air ratio one can notice that in general the increase of CR from 12 to 16 results in an increase of indicated efficiency, while further increase to 18 results in decrease of efficiency in most cases. This decrease in efficiency is the consequence of the higher

thermal losses caused by the higher in-cylinder temperature as well as the higher influence of crevices since the in-cylinder pressure at top dead center (TDC) is higher. By looking at overall results across engine speed range the best indicated efficiency is obtained with  $\lambda = 1.2$  and CR = 16.

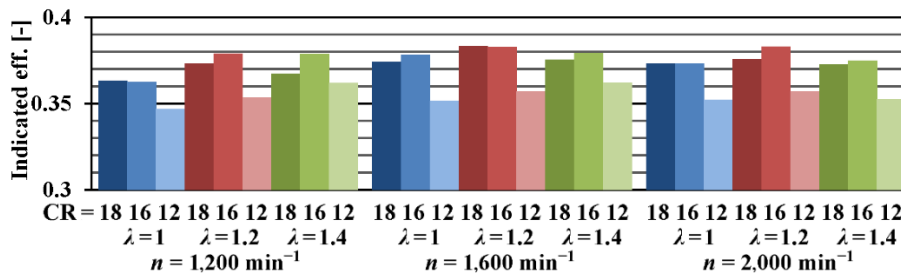


Figure 6. Indicated efficiency in dependence of CR, lambda and engine speed

Figure 7 shows the rate of heat release (RoHR) for optimized spark timing with respect to the highest indicated efficiency for  $\lambda = 1$  and  $\lambda = 1.2$  at  $1,600 \text{ min}^{-1}$ . It can be observed that the increase of compression ratio results with higher peak RoHR values which will lead to larger pressure rise rates and noise, while the increase of lambda value decreases peak RoHR. It can also be observed that optimal points that have lower peak RoHR also have advanced combustion timing, which means that for optimum operation as the combustion intensity is decreased the combustion phasing has to be advanced.

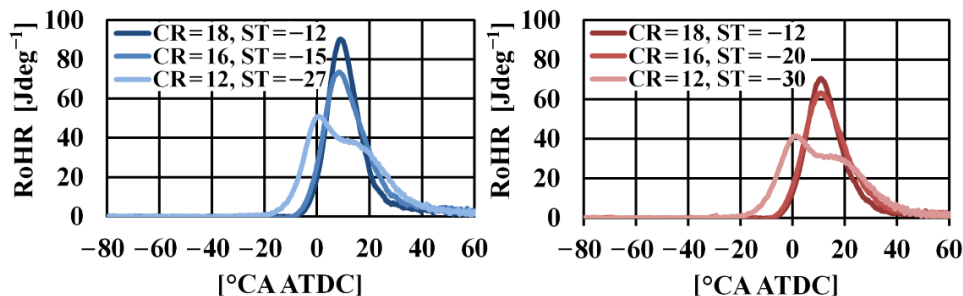


Figure 7. RoHR at  $\lambda = 1$  (left) and  $\lambda = 1.2$  (right) at  $1600 \text{ min}^{-1}$

The changes of harmful exhaust gas emissions (THC, CO and  $\text{NO}_x$ ) of the optimal operating points are shown in fig. 7, 8, 9 and in order to put these results into a context of regulations tab. 2 shows currently valid European Union (EU) standard for allowed exhaust emissions of heavy-duty engines. The regulation prescribes values for steady-state test cycle [world harmonised stationary cycle (WHSC)] for CI engines and transient test cycle [world harmonised transient cycle (WHTC)] for spark ignited [positive ignition (PI)] and for CI engines. In this research the SI engine was used in steady state conditions. Since there is no regulation for that engine in those conditions the WHTC (PI) limits will be used as reference for this work, keeping in mind that limits are slightly higher for WHTC than for WHSC.

Figure 7 shows measured values of THC expressed in g/kWh. It can be noticed that in stoichiometric and slightly lean cases the increase of engine speed results in slight decrease of THC emissions. This could be related to fuel slip since in [20] it was shown that higher

amount of fuel slip is obtained at 1,000 and 1,500 rpm compared to higher engine speeds on the same engine. With constant compression ratio the increase of excess air ratio results in non-monotonic change in THC emission. The change from  $\lambda = 1$  to  $\lambda = 1.2$  results in slight decrease or no change in THC emissions, while further change from  $\lambda = 1.2$  to  $\lambda = 1.4$  results in significant increase in THC emissions. This is caused by slower flame propagation and earlier quenching of the flame in significantly leaner mixtures. At constant excess air ratio the increase of CR in most of the cases results in slight increase in THC emissions. This is probably related to the larger fraction of air/fuel mixture being pushed into the crevices at higher CR. In all of the cases the values of THC are higher than the limits shown in tab. 2 (NMHC + CH<sub>4</sub> = 0.66 g/kWh). The excess of values range from 50% to 10 times more which means that some form of after treatment would be required for satisfying limits in these conditions.

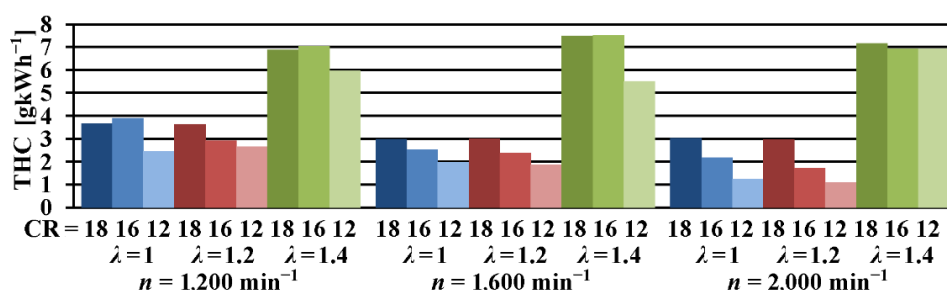


Figure 8. THC (g/kWh) emission in dependence of CR, lambda and engine speed

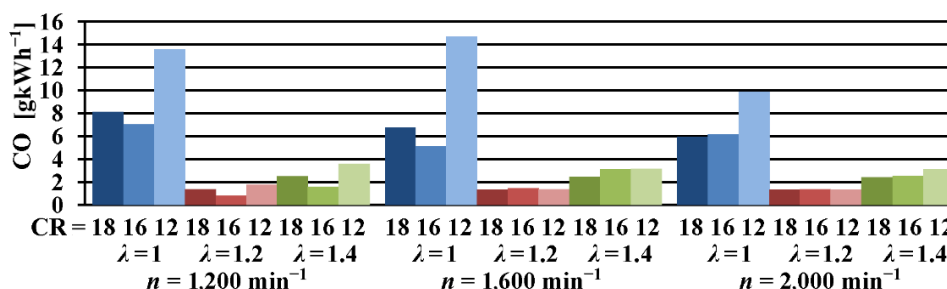


Figure 9. CO emission in dependence of CR, lambda and engine speed

Table 2. Heavy-duty European exhaust emissions standard – Euro VI [19]

	CO [mgkWh <sup>-1</sup> ]	THC [mgkWh <sup>-1</sup> ]	NMHC [mgkWh <sup>-1</sup> ]	CH <sub>4</sub> [mgkWh <sup>-1</sup> ]	NO <sub>x</sub> [mgkWh <sup>-1</sup> ]	NH <sub>3</sub> [ppm]	PM mass [mgkWh <sup>-1</sup> ]	PM number [#kWh <sup>-1</sup> ]
WHSC (CI)	1,500	130	–	–	400	10	10	8 × 10 <sup>11</sup>
WHTC (CI)	4,000	160	–	–	460	10	10	6 × 10 <sup>11</sup>
WHTC (PI)	4,000	–	160	500	460	10	10	Not confirmed yet

The measured CO emission is presented in fig. 8. With constant excess air ratio the increase of compression ratio from 12 to 16 results in lower CO emission. This is caused by the higher in cylinder temperatures obtained with higher compression ratios. Further increase of compression ratio from 16 to 18 results with higher CO emission at low engine speed and with almost equal CO emission as in CR = 16 at middle and higher engine speed. The in-



crease of CO emission with further increase of CR is probably determined by the whole hydrocarbon oxidation process where higher CR results with slightly higher THC caused by larger fraction of mixture pushed into the crevices, and later in the expansion process some of these hydrocarbons form CO but do not fully react to CO<sub>2</sub>. At higher engine speed the CO-CO<sub>2</sub> process is enhanced by the overall higher temperature of the engine and therefore this pathway is not that influential.

With constant CR the increase of excess air ratio from  $\lambda = 1$  to  $\lambda = 1.2$  results in lower CO emissions. This is caused by the CO-CO<sub>2</sub> oxidation pathway which is enhanced by the increased concentration of O<sub>2</sub>. Further increase of excess air ratio from  $\lambda = 1.2$  to  $\lambda = 1.4$  results in slight increase of CO emission. This increase is smaller than the change when excess air ratio changed from 1 to 1.2, and is probably caused by the lower in-cylinder temperature and therefore more advanced quenching and stopping of CO-CO<sub>2</sub> oxidation with smaller change on the side of formation of CO from hydrocarbons. The observed behaviour of the CO emissions with respect to changes in excess air ratio is completely in line with the behaviour shown in literature [8, 21].

The values of CO emissions are higher than the limits defined in tab. 2. With stoichiometric mixture the CO emissions are 1.5-10 times higher depending on the other conditions and on the value of the limit (WHTC or WHSC). In lean conditions the values range from satisfying the limit to 3 times higher values. In any case it seems that the use of oxidation catalyst would be required to satisfy the CO emissions. Since the exhaust gas temperatures are above 396 °C in all measured cases it is expected that the conversion efficiency of 92% is enough to put CO emissions below the limits [22].

The results of NO<sub>x</sub> emissions are shown in fig. 9. With constant CR the lowest NO<sub>x</sub> emissions are achieved with excess air ratio  $\lambda = 1.4$ . In these cases the in-cylinder temperatures are lowest and therefore the formation of NO<sub>x</sub> is reduced (fig. 10). With excess air ratio  $\lambda = 1.2$  the NO<sub>x</sub> formation is highest since the temperature is higher and there is enough oxygen to form NO<sub>x</sub>. On the other hand, although with stoichiometric mixture the temperature is even higher than at  $\lambda = 1.2$  the formation of NO<sub>x</sub> is limited by the lack of oxygen and therefore the emission of NO<sub>x</sub> is lower. But, if compared to the very lean operation  $\lambda = 1.4$ , stoichiometric operation still results with higher NO<sub>x</sub> emission.

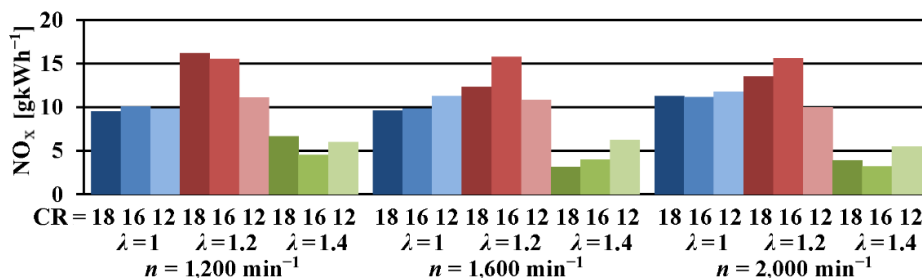


Figure 10. NO<sub>x</sub> emission in dependence of CR, lambda and engine speed

At constant excess air ratio and different CR trends are diverse. The only clear and visible trend is in a change of CR from 12 to 16 at  $\lambda = 1.2$  where the NO<sub>x</sub> emissions increase significantly. All other changes are small and without any trend, although the trends in peak temperatures are quite uniform, higher CR results with higher peak temperature. Peak in-cylinder temperature shown in fig. 11 is calculated from the average temperature of the cylin-

der. Although the temperature of the burned zone is the one that influences  $\text{NO}_x$  formation, the average temperature also indicates the temperature of the burned zone since an increase of the burned zone temperature will lead to the increase of the average temperature as well. At stoichiometric conditions the change of CR almost has no influence on  $\text{NO}_x$ . This can be explained by the fact that although the  $\text{NO}_x$  formation with increase of CR from 12 to 16 is higher ( $\text{NO}_x$  in ppm is larger), the produced power is also larger and therefore the emissions in g/kWh are almost the same. At  $\lambda = 1.4$  the change of CR results with non-monotonic change in  $\text{NO}_x$  emission and the interesting thing is that the emissions does not follow the peak temperature trend. In most of the cases it follows the opposite trend, where with increased peak temperature the emissions are lower. Since the  $\text{NO}_x$  is formed in the burned part of the cylinder and the average temperature in these cases are below 1,800 K (the temperature threshold for  $\text{NO}_x$  formation) the combustion profile determines the  $\text{NO}_x$  emissions. As can be seen in CA50 plot shown in fig. 12, the trend of change of  $\text{NO}_x$  emission with the change of CR at  $\lambda = 1.4$  corresponds to combustion timing, with later timing producing lower  $\text{NO}_x$ .

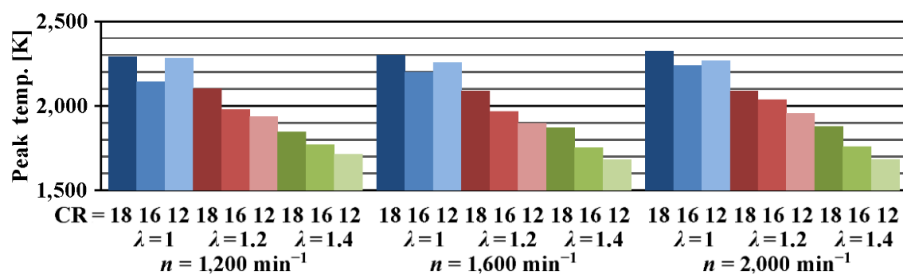


Figure 11. Peak in-cylinder temperature

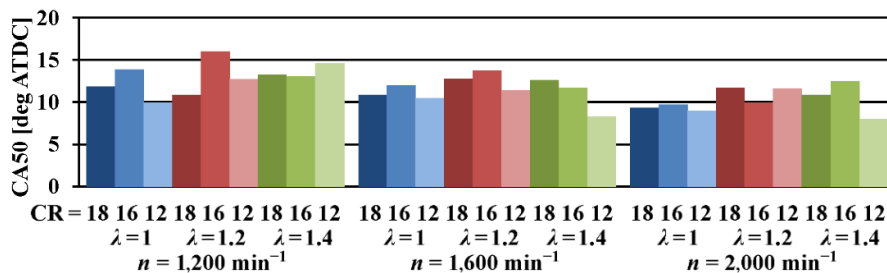


Figure 12. CA50 in dependence of CR, lambda and engine speed

All measured values of  $\text{NO}_x$  are significantly higher (6.8-35 times) than the allowed values (0.46 g/kWh) set by the EU standard (tab. 2) which means that the engine in these conditions would still need some after treatment. In stoichiometric conditions the three way catalyst could be used and in these conditions the conversion of 95% would be required which is achievable with today's catalysts [23]. In lean conditions the required efficiency is slightly lower (92%) and can also be achieved with today's  $\text{NO}_x$  after treatment devices for lean burn engines.

## Conclusions

In presented study, the effects of compression ratio, excess air ratio and engine speed on the performance and emissions of natural gas fuelled spark ignition engine are ex-

amined. The main objective of the work was to show the advantages and disadvantages of using different compression ratio, especially high compression ratios similar to diesel engine. The main conclusions of the paper are:

- indicated efficiency of spark ignited natural gas fuelled engine is highly influenced by CR; there is some influence of lambda and engine speed, but the influence of CR is greater with indicated efficiency increasing as the CR increases from 12 to 16; further increase of compression ratio leads to decrease of indicated efficiency because of higher thermal losses and higher influence of crevices,
- increasing of compression ratio decreases ignition delay and combustion duration mainly as a consequence of different spark timings,
- IMEP is higher at lower engine speeds because of the influence of volumetric efficiency,
- the THC emission is highest at lean mixture ( $\lambda = 1.4$ ) which is caused by slower in-cylinder flame propagation, lower temperature and probably flame quenching; the increase of compression ratio also increases THC emission which is caused by higher influence of crevices; at stoichiometric or slightly lean conditions ( $\lambda = 1.2$ ) the influence of CR on THC emissions is significant, but the change to  $\lambda = 1.4$  significantly increases THC regardless of the CR,
- although there is some influence of CR on CO emission (the increase from CR = 12 to CR = 16 results in decrease of CO emission, while further increase to CR = 18 slightly increases CO), the dominant factor in CO emissions is excess air ratio; the change of operation from stoichiometric to slightly lean results in significant decrease of CO emissions, and
- the emissions of NO<sub>x</sub> are also significantly influenced by excess air ratio and much less by compression ratio, except for  $\lambda = 1.2$  where CR has strong influence on NO<sub>x</sub>; in lean operation the NO<sub>x</sub> emission is not exclusively correlated to peak cylinder temperatures, but depends on full combustion profiles; for operation without catalyst the excess air ratio should be even higher than  $\lambda = 1.4$ , which is not possible with this type of ignition system.

With all the above highlighted conclusions, there are three possible modes of operation that would require different hardware in satisfying emission regulations. The stoichiometric mixture provides the highest engine power with drawbacks in exhaust emissions and efficiency, but the emissions can be eliminated with relatively cheap three way catalyst. Lean burn with  $\lambda = 1.2$  achieves the highest indicated efficiency and reduces THC and CO exhaust emissions, however the engine would still require oxidation catalyst and a lean burn NO<sub>x</sub> catalyst. Finally, the operation with  $\lambda$  higher than 1.4 would probably reduce NO<sub>x</sub> below legal limits but would require oxidation catalyst and the ignition system which provides higher source of energy. In all the cases the favourable CR is much higher than the usual compression ratio of SI engines and is equal to CR = 16.

#### Acknowledgment

The study was performed within the FMENA project “Experimental Research, Optimization and Characterization of piston engine operation with DUAL-Fuel Combustion – DUFOROC” IP-2014-09-1089 funded by the Croatian Science Foundation. This help is gratefully appreciated.

#### Nomenclature

- $n$  – engine speed, [min<sup>-1</sup>]
- $V$  – displacement, [cm<sup>3</sup>]

Greek symbols		CI	– compression ignited
$\lambda$	– air excess ratio, [–]	CH <sub>4</sub>	– methane
$\varphi$	– air equivalence ratio, [–]	CR	– compression ratio, [–]
Acronyms		HC	– hydrocarbon
AC	– alternating current	IC	– internal combustion
AFR	– air to fuel ratio	IMEP	– indicated mean effective pressure, [bar]
ATDC	– after top dead centre	MBT	– spark timing for max. brake torque
BSFC	– brake specific fuel combustion	NH <sub>3</sub>	– ammonia
CA	– crank angle	NMHC	– non-methane hydrocarbon
CA <sub>x</sub>	– the crank angle at which <i>x</i> % of total heat release occurs, [°CA ATDC]	NO <sub>x</sub>	– nitrous oxide, [gkWh <sup>-1</sup> ]
CI	– compression ignited	PI	– positive ignition
CH <sub>4</sub>	– methane	PM	– particulate matter
CNG	– compressed natural gas	RoHR	– rate of heat release
CO	– carbon monoxide, [gkWh <sup>-1</sup> ]	SI	– spark ignited
CO <sub>2</sub>	– carbon dioxide	ST	– spark timing
CoV	– coefficient of variation	WHSC	– steady-state test cycle
		WHTC	– transient test cycle
		WOT	– wide open throttle

## References

- [1] Taritaš, I., *et al.*, The Effect of Operating Parameters on Dual Fuel Engine Performance and Emissions – An Overview, *Trans FAMENA*, 41 (2017), 1, pp 1-14
- [2] Khan, M. I., *et al.*, Technical Overview of Compressed Natural Gas (CNG) as a Transportation Fuel, *Renew. Sustain. Energy Rev.*, 51 (2015), Nov., pp. 785-797
- [3] Serrano, D., Bertrand, L., Exploring the Potential of Dual Fuel Diesel-CNG Combustion for Passenger Car Engine, *Proceedings, FISITA 2012 World Congress*, Beijing, China, 2012
- [4] Tahir, M. M., *et al.*, Performance Analysis of a Spark Ignition Engine Using Compressed Natural Gas (CNG) as Fuel, *Energy Procedia*, 68 (2015), Apr., pp 355-362
- [5] Aslam, M. U., *et al.*, An Experimental Investigation of CNG as an Alternative Fuel for a Retrofitted Gasoline Vehicle, *Fuel*, 85 (2006), 5, pp. 717-724
- [6] Jahirul, M. I., *et al.*, Comparative Engine Performance and Emission Analysis of CNG and Gasoline in a Retrofitted Car Engine, *Appl. Therm. Eng.*, 30 (2010), 14, pp. 2219-2226
- [7] Cho, H. M., He, B.-Q., Spark Ignition Natural Gas Engines – A Review, *Energy Convers. Manag.*, 48 (2007), 2, pp. 608-618
- [8] Korakianitis, T., *et al.*, Natural-gas Fueled Spark-ignition (SI) and Compression-ignition (CI) Engine Performance and Emissions, *Prog. Energy Combust. Sci.*, 37 (2011), 1, pp. 89-112
- [9] Raju, A. V. S. R., *et al.*, Experimental Investigations on a Lean Burn Natural Gas Fuelled si Engine at Different Compression Ratios, *J. Inst. Eng. Mech. Eng. Div.*, 80 (2000), 4, pp. 144-147
- [10] Zhang, Q., *et al.*, Combustion and Emissions of a Euro VI Heavy-duty Natural Gas Engine Using EGR and TWC, *J. Nat. Gas. Sci. Eng.*, 28 (2016), Jan., pp. 660-671
- [11] Zoldak, P., Naber, J., Spark Ignited Direct Injection Natural Gas Combustion in a Heavy Duty Single Cylinder Test Engine – Start of Injection and Spark Timing Effects, SAE Technical Paper, 2015-01-2813, 2015
- [12] Zoldak, P., Naber, J., Spark Ignited Direct Injection Natural Gas Combustion in a Heavy Duty Single Cylinder Test Engine – AFR and EGR Dilution Effects, SAE Technical Paper, 2015-01-2808, 2015
- [13] Lim, G., *et al.*, Effects of Compression Ratio on Performance and Emission Characteristics of Heavy-duty SI Engine Fuelled with HCNG, *Int. J. Hydrogen Energy*, 38 (2013), 11, pp. 4831-4838
- [14] Takagaki, S., Raine, R., The Effects of Compression Ratio on Nitric Oxide and Hydrocarbon Emissions from a Spark-Ignition Natural Gas Fuelled Engine, SAE Technical Paper, 970506, 1997
- [15] Asar, G. M. M., *et al.*, Study of Natural Gas in an Air-Cooled Spark Ignition Engine, SAE Technical Paper, 1997-10-972113, 1997, pp. 291-296
- [16] \*\*\*, Hatz Diesel, <http://www.hatz-diesel.com/en/products/diesel-engines/d-series/1d81/>
- [17] Zhu, G., *et al.*, MBT Timing Detection and its Closed-loop Control Using In-cylinder Pressure Signal, SAE Technical Paper, 2003-01-3266, 2003

- [18] Vuilleumier, D., *et al.*, Intermediate Temperature Heat Release in an HCCI Engine Fueled by Ethanol/n-heptane Mixtures: An Experimental and Modeling Study, *Combust. Flame.*, 161 (2013), 3, pp. 680-695
- [19] \*\*\*, Delphi Technologies, <http://delphi.com/docs/default-source/worldwide-emissions-standards/2016-2017-heavy-duty-amp-off-highway-vehicles.pdf?status=Temp&sfvrsn=0.03636262961639791>
- [20] Sremec, M., *et al.*, Numerical Investigation of Injection Timing and Knock on Dual Fuel Engine, *Proceedings*, 2<sup>nd</sup> SEE SDEWES Conference, Piran, Slovenia, 2016.
- [21] Eswara, A. K., *et al.*, Introduction to Natural Gas: A Comparative Study of its Storage, Fuel Costs and Emissions for a Harbor Tug, Conference Paper, Annual Meeting of Society of Naval Architects & Marine Engineers (SNAME), Bellevue, Washington, United States of America, 2013
- [22] \*\*\*, Nett Technologies Inc., <https://www.nettinc.com/information/emissions-faq/how-does-an-oxidation-catalyst-work>
- [23] Basshuysen, R., Schäfer, F., *Internal Combustion Engine Handbook*, SAE International, Warrendale, Pennsylvania, United States of America, 2004